Proposed antiferromagnetically coupled dual-layer magnetic force microscope tips

John O. Oti, Paul Rice, and Stephen E. Russek
Electromagnetic Technology Division, National Institute of Standards and Technology, Boulder, Colorado 80303

A magnetic force microscope tip designed from dual-layer magnetic films of antiferromagnetically coupled magnetic layers is proposed. A theoretical analysis of the possible advantages of such a tip over conventional single-layer tips is given, using an extension to dual layers of a previously described micromagnetic model of single-layer tips. In contrast to single-layer tips, the magnetic domains of dual-layer tips are less sensitive to the fringing fields of the specimen, and the tips' stray fields are greatly reduced, thus minimizing the likelihood of erasure of the sample magnetization. These properties of dual-layer tips should lead to improved resolution of magnetic force microscopy images.

I. INTRODUCTION

The imaging component of a magnetic force microscope (MFM) system is a probe in the form of a sharp tip mounted at the end of a soft cantilevered spring and positioned near the surface of the specimen. The MFM image is obtained from the force interactions between the tip and specimen. Traditionally, MFM tips have been made from a single magnetic material, and a variety of tip shapes and materials have found practical application.

A MFM tip should remain uniformly magnetized as it interacts with a specimen and not generate large stray fields that inadvertently alter the magnetization pattern of the specimen. The first property helps the interpretation of images, while a contravention of the second property defeats the aim of the imaging process, which is to obtain an image of the magnetization of the specimen without destroying it. In this regard, traditional MFM tips have limited capabilities. Traditional soft magnetic tips, such as nickel with a coercivity H_c of about 40 A/m and a saturation magnetization M_s of about 500 kA/m, are, by virtue of their low coercivities, unsuitable for imaging high-moment films. Their magnetization is usually rendered unstable by the large fringing field of the film surfaces. A hard magnetic tip such as iron ($H_c \approx 160$ kA/m, $M_s \approx 1700$ kA/m), although largely immune to effects of fringing field, can itself generate high enough stray fields to alter the magnetization of soft magnetic films. All this limits the range of applicability of the tips.

We propose a new MFM tip that overcomes these limitations. The new tip is a dual-layer magnetic film, with strongly antiferromagnetically coupled ferromagnetic layers separated by a nonmagnetic layer. Each magnetic layer and the separation layer are a few nanometers thick. Strong antiferromagnetic coupling maintains the stability of oppositely directed domains in the magnetic layers. The resulting magnetic-field-flux closure at the tip edges reduces the tip's stray fields. The tip's stray field pattern leads to improved resolution of MFM images.

We have developed a micromagnetic MFM model to analyze the dual-layer tips. An analysis of the effects of the antiferromagnetic coupling on the response of dual-layer tips is presented in this article. Traditional MFM tips are called simply single-layer tips in the article.

II. MICROMAGNETIC MODEL

The micromagnetic model of the proposed tip is an extension of our previously described single-layer model.[1] The geometry of the dual-layer model for a triangular tip is shown in Fig. 1(a). The tip is scanned at a fixed distance d_0 above the sample from point A to point B. Other tip shapes

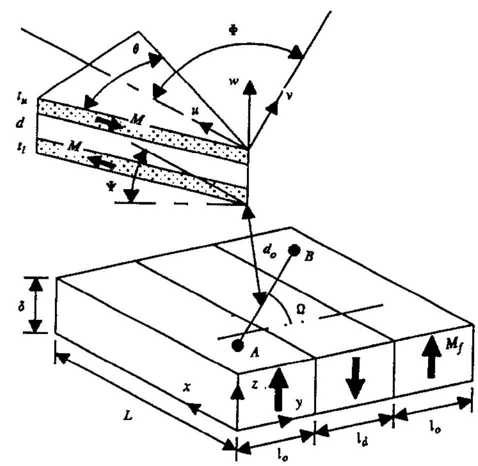

(a)

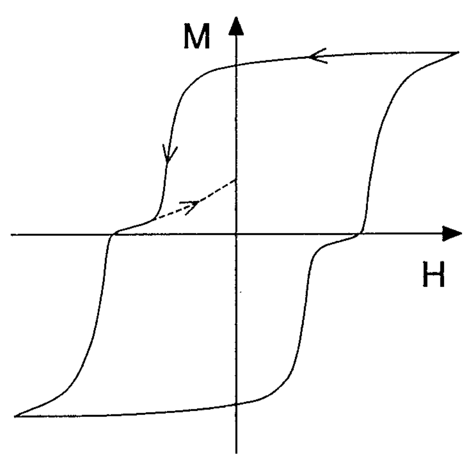

(b)

FIG. 1. (a) Geometry of micromagnetic model, showing defining dimensions and two abrupt Bloch walls. (b) Illustration of the field sequence for obtaining antiferromagnetic coupled bilayers. Arrows indicate the path traversed in the major hysteresis curve of the tip in the v direction.

0021-8979/94/75(10)/6881/3/$6.00

such as bars are possible. A way of traversing the major hysteresis loop which results in the antiparallel orientation of magnetization in the ferromagnetic layers is illustrated in Fig. 1(b). The humps that are formed in the branches of the hysteresis loop are due to the difference in the switching fields of the magnetic layers that is enhanced by the antiferromagnetic coupling between them. Subscripts u and l are used to distinguish between quantities of the upper and lower magnetic layers of the tip in Fig. 1(a). The upper and lower magnetic layers have thicknesses of t_u and t_l, and are separated by a nonmagnetic layer of thickness d. Each magnetic layer is modeled using closely packed discrete elements with rectangular parallelipiped shapes that have square cross sections in the plane of the probe [the u-v plane of Fig. 1(a)]. The elements represent the grains of the tip medium. The grains interact with each other by nearest-neighbor exchange and long-range magnetostatic interactions. The magnetization of the tip can vary, but that of the film is assumed unaffected by its interaction with the tip. A detailed account of modeling the magnetic layers and calculating forces acting on the tip is given in Ref. 1. Antiferromagnetic coupling between the magnetic layers is simulated by introducing a negative interlayer exchange-interaction parameter. The effective exchange interaction field acting on a grain of the upper layer is given by[1,2]

$$H_u = \frac{2A_u}{(M_u D)^2} \sum M_u + \frac{2A'}{(M_u D)^2} M_l, \tag{1}$$

where $A_u \geqslant 0$ is a phenomenological ferromagnetic exchange parameter for the top layer, $A' \leqslant 0$ is a phenomenological interlayer antiferromagnetic-exchange parameter, D is grain size, and M_u, M_l are the magnetization of grains of the upper and lower layers. The first term on the right-hand side of Eq. (1) represents the exchange interactions among grains of the upper layer; the summation is over the nearest neighbors of the grains. The second term of Eq. (1) represents exchange interactions of the upper layer with grains of the lower layer. Interlayer exchange interactions are assumed to occur between grains in corresponding positions in the layers. Positive values of A' could be used when ferromagnetic exchange coupling between the layers is intended. For simplicity it is assumed that the magnetocrystalline anisotropic properties, the magnetization and grain size D are identical for both magnetic layers. The expression for the exchange interaction field in the lower layer is obtained from Eq. (1) by interchanging the roles of the subscripts u and l.

III. SIMULATION RESULTS

The stray field patterns of the dual-layer and single-layer tips, in the active regions of the tips, are compared in Fig. 2. The stray field of the single-layer tip radiates outwardly from the tip toward the sample surface and thus is more likely to affect the magnetization of the sample. The stray field of the dual-layer tip, on the other hand, is localized about the active region due to magnetization flux closure stemming from the proximity of the opposite magnetic poles in the magnetic layers. The force sensitivity of the dual-layer tip is affected by the choice of the layer thicknesses t_u and t_l. In a region of

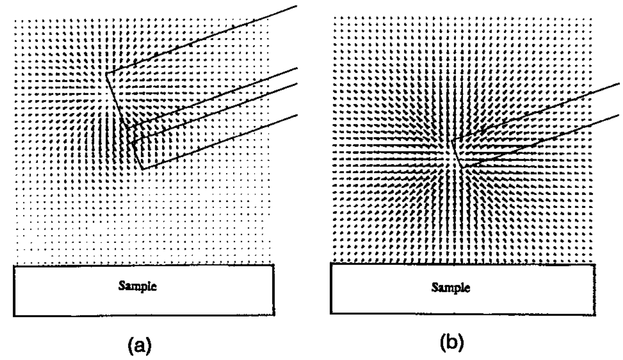

FIG. 2. Longitudinal section (in the u-w plane of Fig. 1) of stray fields for triangular tips for (a) dual-layer tip and (b) single-layer tip.

constant fringing field of the sample, the force acting on a tip of equally thick magnetic layers with a small separation between them is vanishingly small; however, when the layers have the same thicknesses, the tip is sensitive to field gradients. When the tip distance d_0 is less than the layer spacing d, these gradient forces can be nearly as large as the forces acting on a single-layer tip in a uniform field.

Force profiles from a single scan of two abrupt Bloch walls [Fig. 1(a)], for three different antiferromagnetic exchange parameters A', are plotted in Fig. 3. A tip magnetization of $M = 1430$ kA/m and first-order anisotropy constant of $K = 4.3 \times 10^5$ J/m^3, corresponding to those of cobalt,[3] were used in the calculations; magnetic layer thicknesses $t_u = 10$ nm and $t_l = 15$ nm and an interlayer separation $d = 2$ nm were used. An intralayer exchange constant $A = 4 \times 10^{-10}$ J/m, corresponding to a maximum exchange field of 2343 kA/m, was used. The tip was inclined at an angle $\psi = 30°$ to the sample and separated from it by $d_0 = 5$ nm. The tip was scanned normal to the domain wall [$\Omega = 0°$ in Fig. 1(a)]. The same grain sizes, linear dimensions of the tips, and gyromagnetic parameters as in Ref. 1 were used. Each cobalt grain is characterized by a uniaxial magnetocrystalline anisotropy; the anisotropy directions were assigned randomly among the grains in the calculation. The sample

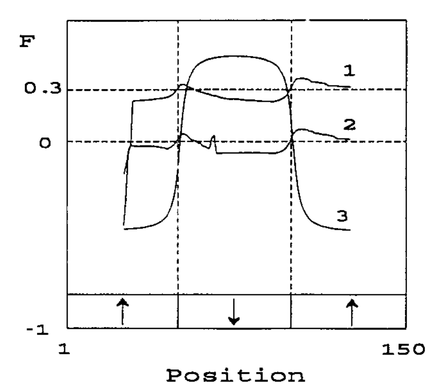

FIG. 3. Profiles of reduced force F as functions of interlayer antiferromagnetic coupling A' for $A' = -4 \times 10^{-11}$ J/m equivalent to an antiferromagnetic coupling field $H_{AF} = 468.5$ kA/m (curve 1), $A' = 0$, $H_{AF} = 0$ (curve 2), and $A' = -2 \times 10^{-10}$ J/m, $H_{AF} = 2343$ kA/m (curve 3). Curve 1 is displaced vertically by 0.3 for clarity.

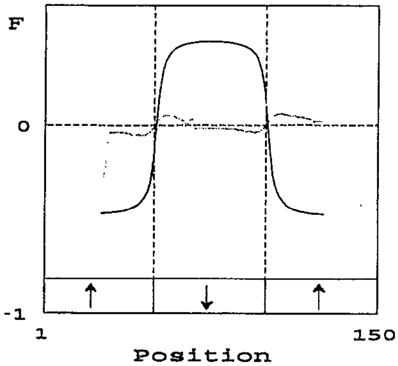

FIG. 4. Force profiles of dual-layer tip with $A'=-2\times10^{-10}$ J/m (solid curve) and single-layer tip (dotted curve).

properties were chosen to correspond to those of a magnetic garnet film described in Ref. 1. The following linear dimensions of the sample were used in the calculations [see Fig. 1(a)]: δ=2000 nm, $l_d=l_0=500$ nm, and $L=1000$ nm.

The antiferromagnetic-coupled state of the magnetic layers is a low-energy state, which requires an external field greater than the antiferromagnetic coupling field to move it away from this state. The force profile is greatly distorted for $A'=0$ and -4×10^{-11} J/m (curves 1 and 2) because the fringing field surpasses the antiferromagnetic coupling field and leads to instability of the magnetic domains. With increasing A' the magnetic domains of the tip gradually stabilize, the force increases, and the force transition regions sharpen (curve 3). Stable tip domains also lead to larger force amplitudes. The calculation was repeated for a single-layer tip using the same shape and mutual orientation of the tip and sample as for the dual-layer tips. The single-layer tip had a thickness equal to the combined thickness of the magnetic layers of the dual-layer tips, and the magnetic properties were the same as those of the magnetic layers of the dual-layer tips. The calculated force profile of the single layer tip is compared with that of a dual-layer tip having $A'=-2\times10^{-10}$ J/m in Fig. 4; the dual-layer tip produces a larger force with a sharper transition region which is better centered and more nearly symmetrical relative to the domain walls. These properties, due to the stability of domains, in the magnetic layers lead to a better spatial resolution of the final MFM image.

IV. DISCUSSION

Strongly antiferromagnetically coupled multilayer magnetic films that are currently receiving a lot of attention in the literature in connection with their giant magnetoresistance properties would make good candidate materials for constructing the dual-layer tips.[4] The range of interlayer separation d corresponding to antiferromagnetic coupling between the magnetic layers is material dependent. An Fe-Cr-Fe system reported in Ref. 4 has a coupling field of 1600 kA/m. The magnitude of the fringing field close to the surface of the film is bounded by the value of the saturation remanent magnetization. The saturation remanent magnetization of metallic recording films,[3] for example, ranges from 400 to 1000 kA/m, which is smaller than the coupling field of the Fe-Cr-Fe system. Thus, a Fe-Cr-Fe probe is expected to remain stable while imaging such films or films with lesser saturation magnetization values. Other coupled multilayers such as Co-Cr-Co, Co-Ru-Co, and Co-Cu-Co multilayers with coupling fields of comparable magnitudes to the Fe-Cr-Fe system have also been reported.[5,6]

[1] J. O. Oti and P. Rice, J. Appl. Phys. **73**, 5802 (1993).
[2] J. O. Oti, IEEE Trans. Magn. **MAG-29**, 1265 (1993).
[3] E. Koster and T. C. Arnoldussen, in *Magnetic Recording I: Technology*, edited by C. D. Mee and E. D. Daniels (McGraw-Hill, New York, 1982), Chap. 3.
[4] R. L. White, IEEE Trans. Magn. **MAG-28**, 2482 (1992).
[5] S. S. Parkin, N. More, and K. P. Roche, Phys. Rev. Lett. **64**, 2304 (1990).
[6] M. A. Howson, B. J. Hickey, J. Xu, and D. Grieg, Phys. Rev. B **48**, 1322 (1993).